Probing the Extremes of Covalency in M–Al bonds: Lithium and Zinc Aluminyl Compounds

Matthew M. D. Roy,[a] Jamie Hicks,[a] Petra Vasko,[a,b] Andreas Heilmann,[a] Anne-Marie Baston,[a] Jose M. Goicoechea*[a] and Simon Aldridge*[a]

Abstract: Synthetic routes to lithium, magnesium and zinc aluminyl complexes are reported, allowing for the first structural characterization of an unsupported lithium-aluminium bond. Crystallographic and quantum chemical studies are consistent with the presence of a highly polar Li–Al interaction, characterized by a low bond order and relatively little charge transfer from Al to Li. Comparison with magnesium and zinc aluminyl systems reveals changes to both the M–Al bond and the (NON)Al fragment (where NON = 4,5-bis(2,6-diisopropylanilido)-2,7-di-tert-butyl-9,9-dimethylxanthene) consistent with greater covalent character, with the latter complex being shown to react with CO_2 via a pathway that implies that the *zinc* centre acts as the nucleophilic partner.

Low-valent main group compounds have attracted significant recent interest, not least by challenging traditional perspectives of electronic structure/bonding and the potential for s/p-block elements to find applications in small molecule activation.[1] Within this sphere, the isolation of molecular Al(I) compounds such as Schnöckel's $(Cp^*Al)_4$[2] and Roesky's $(Nacnac^{Dipp})Al$ (where $Nacnac^{Dipp}$ = $HC(MeCDippN)_2$)[3] offered a counterpoint to the near universal view of aluminium compounds as being Lewis acidic.[4] More recently these systems have also found extensive use in the activation of small molecules, making use of the ready propensity of the aluminium centre to undergo oxidative addition and related processes.[5]

By contrast, the related development of Al(I) systems of the type $[AlR_2]^-$, anionic analogues of N-heterocyclic carbenes, lagged behind the other elements of group 13, reflecting (at least in part) the lower electronegativity of aluminium.[6] Examples of formally anionic boryl[7] and gallyl[8] systems of this type were reported as long ago as 2006 and 1999, respectively, while the first structurally characterized aluminyl system was not reported until 2018.[9-11] Since this time, a number of other aluminyl systems have been reported, featuring a range of supporting R substituents (Figure 1). To date, all of these have been generated as K^+ salts, reflecting the widespread efficacy of potassium reductants in generating such highly reduced species.

Even within this relatively small set of compounds, the nature of the supporting substituents has been shown to have a profound effect on key orbital energies, in particular based on the degree of π-donor stabilization of the formally vacant pπ orbital at Al.[12] As such, a number of these systems have been shown to possess a narrow energy separation between σ and π symmetry frontier orbitals (superficially the HOMO and LUMO) and to display unusual/unprecedented patterns of reactivity, for example involving the cleavage of C–H and C–C bonds of simple unactivated hydrocarbons.[9,10b,10e,13] An alternative strategy to modulate the reactivity profiles of anionic Al(I) compounds (e.g. as nucleophiles or as reducing agents) is to vary the identity of the 'partner' metal, and through it the degree of charge separation and associated hard/soft character at Al. Studies to date hint that the nature of the counter-cation can have a noticeable effect on reactivity at the aluminium centre.[9,10e,13,14] Of systems reported to date, only two are accessible as separated ion pairs featuring the effectively 'naked' aluminyl anion, with the K^+ cation having been sequestered by the use of a cryptand or crown ether ligand.[10c,13] Cation exchange has been touched upon in the synthesis of aluminyl compounds featuring Mg,[9,10d] Ca,[10d] Au,[15] Y[16] or Cu[17] partners, but to our knowledge no other alkali metal aluminyl compounds have been reported.

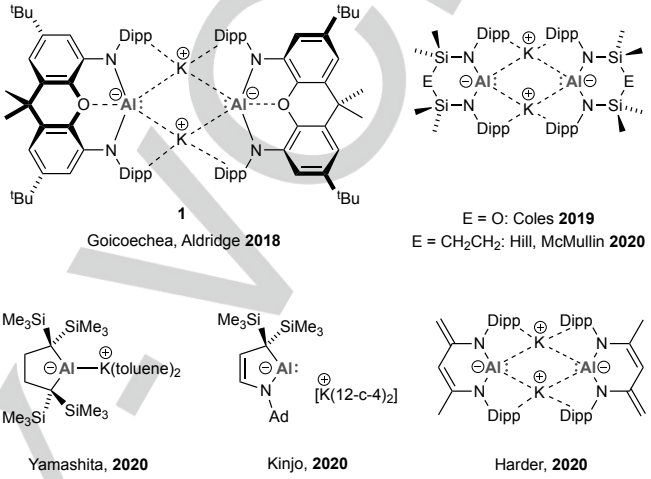

Figure 1. Recently reported examples of aluminyl systems supported by potassium counterions. (Dipp = 2,6-diisopropylphenyl; 12-c-4 = 12-crown-4)

With this in mind, in the current manuscript we report on novel synthetic routes to lithium, magnesium and zinc aluminyl systems - the former representing the first example of a compound featuring a direct lithium-aluminum bond. With these compounds in hand, we present a systematic appraisal of the effects of the partner metal on the nature of the M–Al bond through crystallographic, computational and reactivity studies.

[a] Dr M.M.D. Roy, Dr. J. Hicks, Mr. A. Heilmann, Ms A. Baston, Dr P. Vasko, Prof. J.M. Goicoechea, Prof S. Aldridge
Inorganic Chemistry Laboratory, Department of Chemistry, University of Oxford, South Parks Road, Oxford, OX1 3QR, UK
E-mail: simon.aldridge@chem.ox.ac.uk
Dr. P. Vasko
Department of Chemistry, Nanoscience Center, University of Jyväskylä, P.O. Box 35, Jyväskylä, Finland, FI-40014

Supporting information for this article is given via a link at the end of the document. Structural data has been deposited with the CCDC (refs: 2095877-2095879)

Two synthetic approaches have been probed with the intention of expanding the range of accessible aluminyl compounds featuring a xanthene-derived NON backbone. These involved either the use of aluminium iodide precursor (NON)AlI (**2**) and alternative reducing agents (alkali metals, Mg(I); Scheme 1), or metathesis chemistry employing the existing (dimeric) potassium aluminyl compound $K_2[(NON)Al]_2$ (**1**) and electrophilic sources of the second metal (Scheme 2).

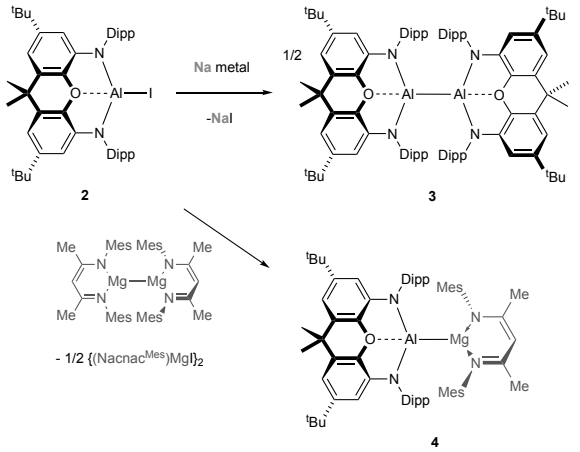

Scheme 1. Chemistry of (NON)AlI (**2**) in the presence of selected reducing agents: syntheses of Al(II) dimer **3** and magnesium aluminyl complex **4**.

In the case of the reactions of **2** with the group 1 metals, lithium and sodium, no evidence is found for the formation of the corresponding Li/Al or Na/Al containing compounds using the reduction approach. While the use of lithium metal leads to cleavage of the supporting Al–N bonds, sodium metal (even in excess) offers a convenient synthesis of the Al(II) dimer $[(NON)Al]_2$ (**3**; 60% isolated yield).[9] *In situ* NMR measurements indicate the formation of the hydride (NON)AlH[9] as a minor side-product in a ca. 1:8 ratio. Isolated samples of **3** can be shown to be resistant to further reduction chemistry (in the presence of either Na or K metals or KC_8), and it is therefore proposed that the formation of potassium aluminyl compound **1** from (NON)AlI (**2**) does not proceed via **3** as an intermediate. Accordingly, the reaction of **2** with one equivalent of KC_8 in benzene-d_6 solution generates (after 2 h) a 1:1 mixture (in terms of aluminium centres) of potassium aluminyl **1** and unreacted Al(III) iodide **2**. Over a period of 16 h at room temperature this mixture is converted slowly into the Al(II) system **3**. The corresponding 1:1 reaction between isolated samples of **1** and **2** also gives **3**,[9] implying that the Al–Al bond forming process is heterolytic, i.e. involving coupling of nucleophilic/electrophilic aluminium components. The implications of this experiment are that Al–Al bond formation is slow (presumably on steric grounds), and that single electron transfer from the potassium graphite reductant to the putative first-generated $[(NON)Al]^{\cdot}$ radical is relatively fast - such that competing homolytic dimerization (to give **3**) or H-atom abstraction from the solvent (to give (NON)AlH) is not observed under these conditions to any significant extent. In the case of the sodium metal reduction, the second single electron transfer step is presumably slower (potentially due to surface area effects); no significant amounts of Al(I) products are observed - but rather **3** and (NON)AlH resulting from alternative reactions of the first formed $[(NON)Al]^{\cdot}$ radical.

With this in mind we were also keen to investigate the reactivity of **2** with Jones' reagent, $[(Nacnac^{Mes})Mg]_2$ (where $Nacnac^{Mes}$ = $HC(MeCMesN)_2$) which has been shown to be a convenient (and soluble) two-electron reductant in hydrocarbon solution.[18] Accordingly, the reaction of **2** with slightly greater than one equivalent of the $[(Nacnac^{Mes})Mg]_2$ dimer in toluene solution at 80°C is shown to proceed smoothly, yielding the magnesium aluminyl compound $(Nacnac^{Mes})MgAl(NON)$ (**4**) in ca. 90% isolated yield. While **4** has previously been reported from the metathesis reaction of potassium aluminyl **1** with $(Nacnac^{Mes})MgI(OEt_2)$,[9] this one-step protocol offers significantly improved overall yields from the common iodide precursor **2** (ca. 90% vs. 65%).

Metathesis chemistry has previously been shown to offer a viable route to the construction of M–Al bonds from aluminyl nucleophiles.[9,10d,15-17] On the other hand, such an approach has not been widely applied for the formation of related derivatives featuring more electropositive metals, such as lithium. Nonetheless, we find that the reaction of potassium compound **1** with lithium iodide in diethyl ether provides access to the desired lithium aluminyl compound $(Et_2O)_2LiAl(NON)$ (**5**; Scheme 2).[19] **5**

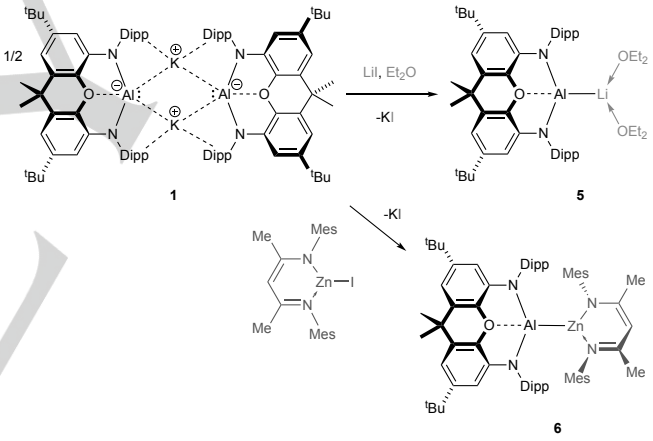

Scheme 2. Synthesis of lithium and zinc aluminyl complexes **5** and **6** via metathesis chemistry utilizing the potassium aluminyl nucleophile **1**.

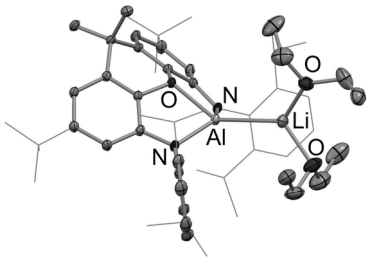

Figure 2. Molecular structure of **5** in the solid state as determined by X-ray crystallography. Hydrogen atoms and solvent molecule omitted and selected substituents shown in wireframe format for clarity. Thermal ellipsoids set at the 40% probability level. Key bond lengths (Å) and angles (°): Al–Li 2.750(4), Li–O 1.912(4), 1.948(4), Al–N 1.961(2), 1.974(2), Al–O 2.114(2), N–Al–N 121.9(1), torsion angles between NC_2 and AlN_2 planes 54.1, 62.0.

is extremely reactive - accounting for the low isolated yield (ca. 20%), but has been characterized by multinuclear NMR and elemental microanalysis and its structure in the solid state confirmed by X-ray crystallography (Figure 2).

The structure of **5** confirms that it is monomeric in the solid state, featuring a single Li–Al contact, and a three-coordinate lithium centre ligated by two additional Et_2O ligands. The associated metal-metal distance (2.750(4) Å) is significantly longer (ca. 10.4 %) than the sum of the respective covalent radii (2.49 Å),[20] hinting at a strong electrostatic contribution to the overall Li–Al interaction (see below). The monomeric nature of **5** contrasts with the dimeric structure observed for potassium compound **1** (which features K···Al and K···arene contacts in the ranges 3.844(1)/4.070(1) and 3.226(3)-3.474(3) Å, respectively).[9] This structural dichotomy finds close precedent in related boryl complexes, with the direct M–B contacts observed for lithium systems,[7,21] contrasting with the dimeric, K···arene bridged structure determined for the potassium analogue.[22] By means of additional comparison, the Li–B bond lengths measured for lithium boryl complexes typically fall 0.1-0.15 Å (4.7-7.1 %) outside of the sum of the respective covalent radii (2.12 Å).[7,20,21]

With mononuclear lithium and magnesium aluminyl compounds in hand (together with the effectively 'naked' $[(NON)Al]^-$ system within the separated ion pair [K(2.2.2-crypt)][Al(NON)]),[13] we sought to expand further the scope of hard/soft and ionic/covalent character available to metal aluminyl compounds via the synthesis of a related system featuring a zinc-aluminium bond. Accordingly the reaction of **1** with $(Nacnac^{Mes})ZnI$[23] in toluene at room temperature allows access to $(Nacnac^{Mes})ZnAl(NON)$ (**6**) in ca. 75% isolated yield (Scheme 2). **6** is obtained as a pale yellow crystalline material, and has been characterized by multinuclear NMR, elemental microanalysis and single crystal X-ray diffraction (Figure 3).

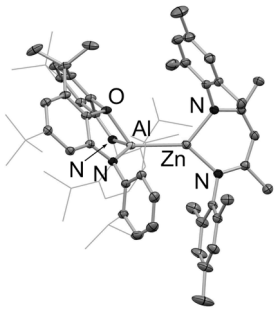

Figure 3. Molecular structure of **6** in the solid state as determined by X-ray crystallography. Hydrogen atoms and solvent molecule omitted and selected substituents shown in wireframe format for clarity. Thermal ellipsoids set at the 40% probability level. Key bond lengths (Å) and angles (°): Al–Zn 2.4678(6), Zn–N 1.994(2), 1.987(2), Al–N 1.894(2), 1.911(2), Al–O 1.975(1), N–Al–N 127.2(1), torsion angles between NC_2 and AlN_2 planes 77.5, 59.5.

While Li–Al contacts of the type found in **5** have no significant literature precedent,[24] Zn–Al covalent bonds have previously been reported, albeit only in a small number of compounds, and all synthesized via a different approach - involving the insertion of neutral Al(I) compounds such as $(Nacnac^{Dipp})Al$ or $(Cp^*Al)_n$, into Zn–X bonds (X = $N(SiMe_3)_2$,[25] Et,[26] Br,[27] or H[28]). The metal-metal bond lengths determined for these compounds fall within a tight range (2.448(2)-2.491(1) Å), and that for **6** (2.468(1) Å) is consistent with these systems.

Table 1: Key bond distances (in Å) determined crystallographically for metal aluminyl compounds **3**, **4**, **5** and **6** (featuring 'terminal' M–Al interactions), together with the 'naked' aluminyl anion $[(NON)Al]^-$.

M	Σr_{cov}/Å[20]	χ[6]	*d*(M–Al)/Å	*d*(Al–O)/Å	*d*(Al–N) /Å
none[a]	-	-	-	2.175(1)	2.022(1) 2.049(1)
Li (**5**)	2.49	0.98	2.750(4)	2.114(2)	1.961(2) 1.974(2)
Mg (**4**)[9]	2.62	1.31	2.696(1)	1.992(1)	1.904(1) 1.918(2)
Al (**3**)[9]	2.52	1.61	2.646(1)	1.976(1) 1.983(1)	1.896(2) 1.900(2) 1.901(2) 1.902(2)
Zn (**6**)	2.43	1.65	2.468(1)	1.975(1)	1.894(2) 1.911(2)

[a] Data taken from the structure of the ion pair [K(2.2.2-crypt)][Al(NON)] which features no K···Al contacts shorter than 5 Å.[13]

The X-ray crystallographic studies carried out on [K(2.2.2-crypt)][Al(NON)] and on compounds **3**-**6** (Table 1) allow some generalizations to be made about geometric structure in these systems as a function of the metal M. Most notably, the transition from Li to Mg to Zn is associated with M–Al bonds which more closely approach the sum of the respective covalent radii, as would be expected on the basis of the Pauling electonegativites of the metals concerned (Li: 0.98; Mg: 1.31; Zn 1.65; cf. Al 1.61).[6] The measured M–Al separations are, respectively 10.4, 2.9 and 1.6% greater than the sum of the covalent radii for the Li, Mg and Zn derivatives **5**, **4** and **6**.[20,29] Increasing covalency in the M–Al bond, and the associated withdrawl of electron density from the aluminium centre also brings about noticeable changes in the geometry of the supporting NON ligand scaffold. Thus, a steady contraction in the Al–O distance associated with the secondary xanthene ether donor is observed (from 2.175(1) to 1.975(1) and 1.976(1)/1.983(1) Å) from the most 'ionic' [K(2.2.2-crypt)][Al(NON)], to the most 'covalent' derivatives, **3** and **6**, complementing the shift of electron density from aluminium into the M–Al bond. A similar contraction (ca. 6.5 %) is measured for the amido Al–N distances, implying a sequentially more positive partial charge at Al.

With a view to rationalizing these structural changes, we sought to obtain a more in depth understanding of the nature of the M–Al bonds in compounds **3**, **4**, **5** and **6** through quantum chemical methods (see Table 2 and ESI). The geometries calculated for each of these complexes and the 'naked' anion $[(NON)Al]^-$[13] agree well with the structures determined by X-ray crystallography. In the case of the unprecedented lithium aluminyl complex **5**, the HOMO and LUMO (Figure 4) are best described as an orbital of sigma bonding character between Al and Li, and an Al-centred p-orbital, respectively. The Wiberg Bond Index (WBI) for the Li–Al bond is relatively low (0.32), and occupancy of the Li 2s orbital as determined by NAO methods is

also small (0.25 e). Consistently, an Atoms in Molecules (QTAIM) calculation reveals a bond path between Li and Al (Figure 4), albeit one with a relatively low electron density, ρ(r), at the Bond Critical Point (BCP; 0.019 e Å^{-3}).

On transitioning successively from Li to Mg to Zn (Table 2) it is evident that (i) the HOMO is successively stabilized; (ii) the WBIs for the M–Al interactions increase; (iii) the population of the *n*s atomic orbital of the partner metal M is raised; and (iv) the electron density, ρ(r), at the BCP between M and Al increases, as expected on the basis of increasing covalent character of the M–Al bond.

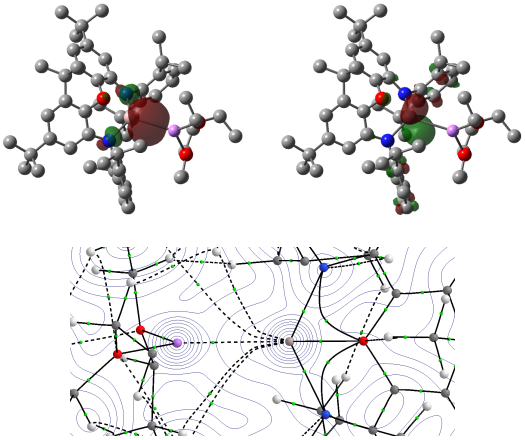

Figure 4. (upper) DFT-calculated HOMO (left, at -4.12 eV, -397 kJ mol^{-1}) and LUMO (right, at -0.05 eV, -5 kJ mol^{-1}) for lithium aluminyl complex **5** using the PBE1PBE hybrid exchange functional and Def2-SVP basis set (MO diagrams are drawn with an isovalue of 0.05 au). (lower) QTAIM analysis of **5** showing bond critical points (BCPs) in green. The values of ρ(r) and ∇^2r(r) at the BCP between Li and Al are 0.019 e Å^{-3} and 0.038 e Å^{-5}, respectively.

Table 2: Orbital energies/separations, Wiberg Bond Indices (WBIs) and NAO-calculated orbital occupancies for complexes **3**, **4**, **5** and **6**.

M	HOMO energy and HOMO-LUMO gap / eV (kJ mol^{-1})	WBI (M–Al)	NAO orbital occupancies	QTAIM ρ(r) at Bond Critical Point (BCP) / e Å^{-3}
Li (**5**)	-4.12 (-397) 4.06 (392)	0.32	Li(2s): 0.25 e	0.019
Mg (**4**)	-5.00 (-483) 4.07 (393)	0.52	Mg(3s): 0.46 e	0.036
Al (**3**)	-6.40 (617)[a] 5.89 (568)[a]	0.91	Al(3s): 0.76 e Al(3p): 0.86 e	0.057
Zn (**6**)	-5.20 (501) 4.32 (417)	0.74	Zn(4s): 0.74 e	0.060

[a] In the case of compound **3** the Al–Al σ-bonding interaction is primarily located in the HOMO-4; data given relate to this orbital.

The NBO-derived natural atomic charges calculated for complexes **3**-**6** and cation-free [(NON)Al]$^-$ are presented in Figure 5. These results are in broad agreement with the results reported by Schoeller and co-workers,[30] which suggest that the predominant resonance structure for anionic aluminium analogues of NHCs features a diamido-stabilized Al$^+$ fragment. Moreover, the variation in the charge distribution within our NON-stabilized aluminyl complexes as a function of partner metal M is in agreement with the structural trends presented in Table 1. As such, increased covalency in the M–Al bond on progressing from Li to Mg to Zn is reflected in increasingly positive natural charges at aluminium, which then provides a rationale for the (experimentally observed) contraction in Al–O and Al–N bond lengths.

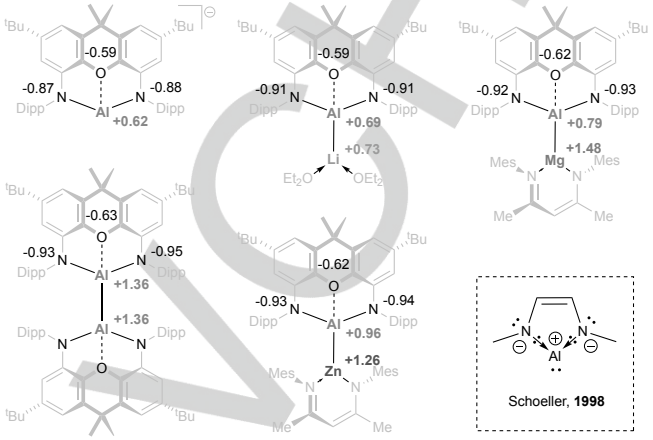

Figure 5. DFT-calculated natural charges for naked aluminyl anion [(NON)Al]$^-$, and the corresponding complexes of lithium, magnesium, aluminium and zinc; (inset) predominant resonance structure proposed by Schoeller and co-workers for a model aluminyl system.[30]

The more covalent nature of the M–Al bond for zinc complex **6** (as reflected in the WBI and NAO orbital occupancies given in Table 2) together with the relatively similar natural charges calculated for the two metal centres (and the very similar electro-negativites of zinc and aluminium),[6] led us to consider experimental methods to probe the bond polarity. In previous work we have used the regiochemistry of insertion of hetero-allenes (such as carbodiimides and carbon dioxide) into a polar Au–Al bond as a probe of the electro-/nucleophilic nature of the two metals.[15] More recently Hill and co-workers have used a similar approach to differentiate between nucleophilic and electrophilic copper centres in copper aluminyl systems featuring different supporting ligand sets.[17] With this in mind, we set out to examine the reactivity of **6** towards similar probe molecules.

In the case of diisopropylcarbodiimide, *in situ* NMR monitoring reveals conversion to a single species, which is characterized by a low-field ^{13}C NMR shift (at δ_C = 200.4 ppm), consistent with conversion of the ^{i}PrNCN^{i}Pr unit into a bent diaminocarbene fragment (cf. δ_C = 219.9 and 220.9 ppm for gold and copper compounds featuring M{C(N^{i}Pr)$_2$}Al motifs).[15,17] In this case, however, the product could not be crystallized - potentially due to the prescence of excess carbodiimide - and so the corresponding reaction with carbon dioxide was targeted in order to provide easier purification and access to definitive structural data. In similar fashion, this reaction leads to the growth of a new ^{13}C NMR signal at δ_C = 219.7 ppm, (cf. δ_C = 242.3 and 234.9 ppm for gold/copper compounds featuring M(CO$_2$)Al units),[15,17] and the product in this case (**7**) could be crystallized from hexane, allowing its identity to be definitively established by multinuclear NMR and analytical methods, and its connectivity to be determined crystallographically (Scheme 3 and Figure 6).

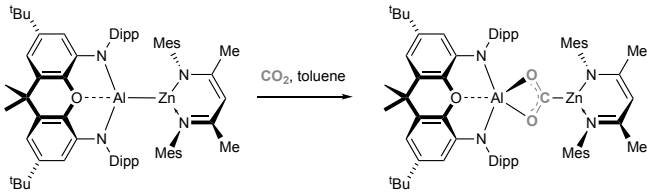

Scheme 3. Insertion of CO_2 into the Zn-Al bond of **6**, establishing regiochemistry consistent with nucleophilic character at zinc.

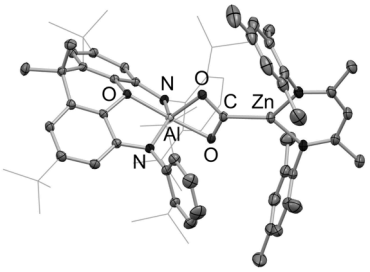

Figure 6. Molecular structure of **7** in the solid state as determined by X-ray crystallography. Hydrogen atoms and solvent molecule omitted and selected substituents shown in wireframe format for clarity. Thermal ellipsoids set at the 40% probability level. Key bond lengths (Å) and angles (°): Zn–C 1.976(2), Zn–N 1.916(2), 1.932(2), C–O 1.302(2), 1.282(2), Al–O 1.876(2), 1.899(1), Al–N 1.869(2), 1.868(2), Al–O_{xanth} 2.011(1), N–Al–N 139.2(1), O–C–O 113.5(2), torsion angles between NC_2 and AlN_2 planes 50.0, 63.9.

The solid-state structure of **7** confirms the regiochemistry of CO_2 insertion implied by spectroscopic measurements, i.e. proceeding via the formation of Zn–C and Al–O bonds, with the zinc centre of **6** formally acting as the nucleophilic partner. The role of steric factors in determining the nature of the insertion process also cannot be ruled out. Geometrically, the AlO_2C four-membered ring resembles closely that found in the related gold compound ($^tBu_3P$)Au(CO_2)Al(NON),[15] while a description of **7** as an (aluminate-backbone supported) carbene complex of zinc is supported by a Zn–C bond length (1.976(2) Å) which is consistent with thse reported for other zinc complexes featuring three-coordinate zinc (e.g. 1.983(4) Å for IMesZn(ODipp)$_2$, where IMes = 1,3-bis(2,4,6-trimethylphenyl)imidazolylidene).[31]

In summary, we present synthetic routes to lithium, magnesium and zinc aluminyl complexes, with the former representing the first structurally characterized example of an unsupported lithium-aluminium bond. Structural and quantum chemical studies are consistent with the presence of a highly polar Li–Al interaction, characterized by a low bond order and relatively little charge transfer from aluminium to lithium. Comparison with related magnesium and zinc systems reveals changes to both the M–Al bond and the (NON)Al fragment consistent with greater covalent character, with the latter complex being shown to react with CO_2 via a pathway that implies that the zinc centre is sufficiently electron rich to formally act as the nucleophilic partner.

Acknowledgements

We thank the Leverhulme Trust (RP-2018-246) for funding aspects of this work. MMDR thanks the Natural Sciences and Engineering Research Council of Canada (NSERC) for a Postdoctoral Fellowship. PV would like to thank the Academy of Finland for financial support (project number 314794) and Prof. Heikki M. Tuononen for providing computational resources.

Keywords: aluminium • aluminyl • low valent compounds • lithium • zinc

[1] See, for example a) P. P. Power, *Nature* **2010**, *463*, 171-177; b) C. Weetmann, S. Inoue, *ChemCatChem.* **2018***, 10*, 4213-4228.

[2] a) C. Dohmeier, C. Robl, M. Tacke, H. Schnöckel, *Angew. Chem. Int. Ed.* **1991**, *30*, 564-565. See also b) S. Schulz, H. W. Roesky, H. J. Koch, G. M. Sheldrick, D. Stalke, A. Kuhn, *Angew. Chem. Int. Ed.* **1993**, *32*, 1729-1731.

[3] C. Cui, H. W. Roesky, H.-G. Schmidt, M. Noltemeyer, H. Hao, F. Cimpoesu, *Angew. Chem. Int. Ed.* **2000**, *39*, 4274-4276.

[4] For other recently-reported neutral Al(I) compounds, see for example: a) P. Bag, A. Porzelt, P. J. Altmann, S. Inoue, *J. Am. Chem. Soc.* **2017**, *139*, 14384-14387; b) S. K. Mellerup, Y. Cui, F. Fantuzzi, P. Schmid, J. T. Goettel, G. Bélanger-Chabot, M. Arrowsmith, I. Krummenacher, Q. Ye, V. Engel, B. Engels, H. Braunschweig, *J. Am. Chem. Soc.* **2019**, *141*, 16954-16960; c) A. Hofmann, C. Pranckevicius, T. Tröster, H. Braunschweig, *Angew. Chem. Int. Ed.* **2019**, *58*, 3625-3629.

[5] a) C. Bakewell, M. Garçon, R. Y. Kong, L. O'Hare, A. J. P. White, M. R. Crimmin, *Inorg. Chem.* **2020**, *59*, 4608-4616; b) A. Dmitrienko, J. F. Britten, D. Spasyuk, G. I. Nikonov, *Chem. Eur. J.* **2020**, *26*, 206-211; c) C. Bakewell, A. J. P. White, M. R. Crimmin, *Chem. Sci.* **2019**, *10*, 2452-2458; d) L. L. Liu, J. Zhou, L. L. Cao, D. W. Stephan, *J. Am. Chem. Soc.* **2019**, *141*, 16971-16982; e) S. Sinhababu, M. M. Siddiqui, S. K. Sarkar, A. Münch, R. Herbst-Irmer, A. George, P. Parameswaran, D. Stalke, H. W. Roesky, *Chem. Eur. J.* **2019**, *25*, 11422-11426; f) A. Paparo, C. D. Smith, C. Jones, *Angew. Chem. Int. Ed.* **2019**, *58*, 11459-11463; g) A. Koner, B. M. Gabidullin, Z. Kelemen, L. Nyulászi, G. I. Nikonov, R. Streubel, *Dalton Trans.* **2019**, *48*, 8248-8253; h) C. Bakewell, B. J. Ward, A. J. P. White, M. R. Crimmin, *Chem. Sci.*, **2018**, *9*, 2348-2356; i) S. Brand, H. Elsen, J. Langer, W. A. Donaubauer, F. Hampel, S. Harder, *Angew. Chem. Int. Ed.* **2018**, *57*, 14169-14173; j) R. Y. Kong, M. R. Crimmin, *J. Am. Chem. Soc.* **2018**, *140*, 13614-13617; k) S. Sinhababu, S. Kundu, A. N. Paesch, R. Herbst-Irmer, D. Stalke, H. W. Roesky, *Eur. J. Inorg. Chem.* **2018**, 2237-2240; l) C. Bakewell, A. J. P. White, M. R. Crimmin, *Angew. Chem. Int. Ed.* **2018**, *57*, 6638-6642; m) L, Tuscher, C. Helling, C. Wölper, W. Frank, A. S. Nizovtsev, S. Schulz, *Chem. Eur. J.* **2018**, *24*, 3241-3250; n) T. N. Hopper, M. Garçon, A. J. P. White, M. R. Crimmin, *Chem. Sci.* **2018**, *9*, 5435-5440.

[6] Pauling electronegativities: B 2.04, Al 1.61, Ga 1.81, In 1.78, Tl 1.62; Li 0.98, Mg 1.31, Zn 1.65. J. Emsley in *The Elements* Oxford University Press, Oxford, 2nd edition, 1991.

[7] Y. Segawa, M. Yamashita, K. Nozaki, *Science* **2006**, *314*, 113-115.

[8] a) E. S. Schmidt, A. Jockisch, H. Schmidbaur, *J. Am. Chem. Soc.*, **1999**, *121*, 9758-9759. See also b) R. J. Baker, R. D. Farley, C. Jones, M. Kloth, D. M. Murphy, *J. Chem. Soc., Dalton Trans.*, **2002**, 3844-3850; c) I. L. Fedushkin, A. N. Lukoyanov, G. K. Fukin, S. Y. Ketkov, M. Hummert, H. Schumann, *Chem. Eur. J.* **2008**, *14*, 8465-8468.

[9] J. Hicks, P.Vasko, J. M. Goicoechea, S. Aldridge, *Nature* **2018**, *557*, 92-95.

[10] a) J. J. Schwamm, M. D. Anker, M. Lein, M. P. Coles, *Angew. Chem. Int. Ed.* **2019**, *58*, 1489-1493; b) S. Kurumada, S. Takamori, M. Yamashita, *Nature Chem.* **2020**, *12*, 36-39; c) K. Koshino, R. Kinjo, *J. Am. Chem. Soc.* **2020**, 142, 9057-9062; d) R. J. Schwamm, M. P. Coles, M. S. Hill, M. F. Mahon, C. L. McMullin, N. A. Rajabi, A. S. S. Wilson, *Angew. Chem. Int. Ed.* **2020**, *59*, 3928-3932; e) S. Grams, J. Eyselein, J. Langer, C. Färber, S. Harder, *Angew. Chem. Int. Ed.* **2020**, *59*, 15982-15986.

[11] For the first structurally authenticated indyl system, see: R. J. Schwamm, M. D. Anker, M. Lein, M. P. Coles, C. M. Fitchett, *Angew. Chem. Int. Ed.* **2018**, *57*, 5885-5887.

[12] For a recent review of aluminyl chemistry, see J. Hicks, P. Vasko, J. M. Goicoechea, S. Aldridge, *Angew. Chem. Int. Ed.* **2021**, *60*, 1702-1713.

[13] J. Hicks, P. Vasko, J. M. Goicoechea, S. Aldridge, *J. Am. Chem. Soc.* **2019**, *141*, 11000-11003.

[14] a) M. Anker, M. P. Coles, *Angew. Chem. Int. Ed.* **2019**, *58*, 18261-18265. See also: b) J. Hicks, A. Heilmann, P. Vasko, J. M. Goicoechea, S. Aldridge, *Angew. Chem. Int. Ed.* **2019**, *58*, 17265-17268.

[15] J. Hicks, A. Mansikkamäki, P. Vasko, J. M. Goicoechea, S. Aldridge, *Nat. Chem.* **2019**, *11*, 237-241.

[16] K. Sugita, M. Yamashita, *Chem.-Eur. J.* **2020**, *26*, 4520-4523.

[17] H. Y. Liu, R. J. Schwamm, M. S. Hill, M. F. Mahon, C. F. McMullin, N. A. Rajabi, *Angew. Chem. Int. Ed.* **2021**, in press (DOI: 10.1002/anie.202104658)

[18] a) S. P. Green, C. Jones, A. Stasch, *Science* **2007**, *318*, 1754-1757; b) C. Jones, *Nat. Rev. Chem.* **2017**, *1*, 0059. For a related use of this Mg(I) system to reductively assemble M–Mg bonds, see for example: c) J. Hicks, C. E. Hoyer, B. Moubaraki, G. Li Manni, E. Carter, D. M. Murphy, K. S. Murray, L. Gagliardi, C. Jones, *J. Am. Chem. Soc.* **2014**, *136*, 5283-5286; d) J. Hicks, E. J. Underhill, C. Kefalidis, L. Maron, C. Jones, *Angew. Chem. Int. Ed.* **2015**, *54*, 10000-10004.

[19] The corresponding reaction of **1** with NaI leads to no apparent conversion, with the unreacted potassium aluminyl being recovered unchanged from the reaction mixture.

[20] B. Cordero, V. Gómez, A. E. Platero-Prats, M. Revés, J. Echeverría, E. Cremades, F. Barragán, S. Alvarez, *Dalton Trans.* **2008**, 2832-2838.

[21] T. Ohsato, Y. Okuno, S. Ishida, T. Iwamoto, K.-H. Lee, Z. Lin, M. Yamashita, K. Nozaki, *Angew. Chem. Int. Ed.* **2016**, 55, 11426–11430.

[22] A. V. Protchenko, P. Vasko, M. A. Fuentes, J. Hicks, D. Vidovic, S. Aldridge, *Angew. Chem. Int. Ed.* **2021**, *60*, 2064-2068.

[23] S. Schulz, T. Eisenmann, D. Schuchmann, M. Bolte, M. Kirchner, R. Boese, J. Spielmann, S. Harder, *Z. Anorg. Allg. Chem.* **2009**, *64*, 1397-1400.

[24] T. Agou, T. Wasano, P. Jin, S. Nagase, N. Tokitoh, *Angew. Chem. Int. Ed.* **2013**, *52*, 10031-10034.

[25] J. Weßing, C. Göbel, B. Weber, C. Gemel, R. A. Fischer, *Inorg. Chem.* **2017**, *56*, 3517-3525.

[26] C. Bakewell, B. J. Ward, A. J. P. White, M. R. Crimmin, *Chem. Sci.* **2018**, *9*, 2348-2356.

[27] A. Paparo, C. D. Smith, C. Jones, *Angew. Chem. Int. Ed.* **2019**, *58*, 11459-11463.

[28] S. Brand, H. Elsen, J. Langer, S. Grams, S. Harder, *Angew. Chem. Int. Ed.* **2019**, *58*, 15496-15503.

[29] The Al–Al distance measured for **3** is longer than would be predicted on the basis of this trend (ca. 5% longer than the sum of the covalent radii). We ascribe this to the very large steric profile enforced by the pair of NON supporting ligands, a finding consistent with ^{1}H NMR studies of **3** which (uniquely among the compounds reported here) features restricted rotation about the M–Al bond at room temperature on the NMR timescale.

[30] a) A. Sundermann, M. Reiher, W. Schoeller, *Eur. J. Inorg. Chem.* **1998**, 305-310. In the case of related boryl systems the partial positive charge at boron is calculated to be much lower, in line with the higher electronegativity of B vs Al: b) Y. Segawa, Y. Suzuki, M. Yamashita, K. Nozaki, *J. Am. Chem. Soc.* **2007**, *130*, 16069-16079.

[31] G. Anantharaman, K. Elango, *Organometallics* **2007**, *26*, 1089-1092.

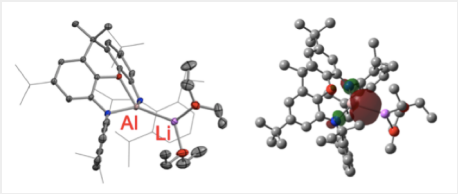

We report the synthesis of the first example of a molecular compound featuring a Li–Al bond, and a systematic analysis of the bonding in this and related Mg and Zn systems through structural, quantum chemical and reactivity probes.

Matthew M. D. Roy, Jamie Hicks, Andreas Heilmann, Anne-Marie Baston, Petra Vasko, Jose M. Goicoechea and Simon Aldridge**

Page No. – Page No.

Probing the Extremes of Covalency in M–Al bonds: Lithium and Zinc Aluminyl Compounds